Efficient calculation of molecular integrals over London atomic orbitals

Tom J. P. Irons, Jan Zemen, and Andrew M. Teale*

School of Chemistry, University of Nottingham, University Park, Nottingham NG7 2RD, United Kingdom

E-mail: andrew.teale@nottingham.ac.uk

Abstract

The use of London atomic orbitals (LAOs) in a non-perturbative manner enables the determination of gauge-origin invariant energies and properties for molecular species in arbitrarily strong magnetic fields. Central to the efficient implementation of such calculations for molecular systems is the evaluation of molecular integrals, particularly the electron repulsion integrals (ERIs). We present an implementation of several different algorithms for the evaluation of ERIs over Gaussian-type LAOs at arbitrary magnetic field strengths. The efficiency of generalized McMurchie-Davidson (MD), Head-Gordon-Pople (HGP) and Rys quadrature schemes is compared. For the Rys quadrature implementation, we avoid the use of high precision arithmetic and interpolation schemes in the computation of the quadrature roots and weights, enabling the application of this algorithm seamlessly to a wide range of magnetic fields. The efficiency of each generalised algorithm is compared by numerical application, classifying the ERIs according to their total angular momenta and evaluating their performance for primitive and contracted basis sets. In common with zero-field integral evaluation, no single algorithm is optimal for all angular momenta thus a simple mixed scheme is put forward, which selects the most efficient approach to calculate the ERIs for each shell quartet. The mixed approach is significantly more efficient than the exclusive use of any individual algorithm.

1 Introduction

In recent years, there has been a great deal of interest in the non–perturbative calculation of molecular energies and properties in the presence of arbitrarily strong magnetic fields.[1–12] Investigations have included the implementation of electronic structure calculations at the Hartree-Fock,[1,8] configuration–interaction,[4] coupled-cluster,[9] coupled-cluster equation of motion[12] and current density-functional[6,10,11] levels of theory. Underpinning the implementations of these methods has been the use of Gaussian type London atomic orbitals[13,14] (LAOs). LAOs consist of standard Gaussian basis functions multiplied by a field-dependent plane-wave phase factor, allowing results independent of gauge-origin to be obtained using finite basis sets.

One of the principle challenges in these calculations is the the evaluation of molecular integrals over LAOs. A number of algorithms have been put forward for the evaluation of electron repulsion integrals (ERIs) over LAOs including generalized Obara–Saika,[15–17] accompanying coordinate expansion,[18,19] Rys quadrature,[8,20,21] and McMurchie–Davidson[1,22–24] schemes. In particular, the McMurchie–Davidson scheme has been employed in the London quantum chemistry program[25] and a version of the Rys quadrature scheme in the Bagel program.[26]

A number of advantageous features for integral schemes to perform non-perturbative calculations with arbitrary strength magnetic fields can be identified. The first of these is that the algorithmic complexity should not be significantly increased over the corresponding zero-field scheme. The second is that they should be applicable to arbitrarily high angular momenta functions, in order to allow sufficient flexibility for the description of anisotropic changes in the electronic structure upon application of a magnetic field. The third feature is that they should be efficient for application to both contracted and primitive functions, since the latter may provide additional basis set flexibility in high field applications.

In common with integral schemes at zero field, no single algorithm can satisfy all of these requirements simultaneously. Indeed, each algorithm inherently has its own strengths and weaknesses; often the most effective approach is to use several algorithms and select the most efficient for each integral class extemporaneously. In this work we explore generalized algorithms based on the McMurchie–Davidson (MD), Head-Gordon Pople (HGP) and Rys quadrature methods.

It has been shown that the generalzed MD algorithm is significantly more complex than the standard equivalent, requiring many more intermediates, thus does not exhibit the same efficiency or scaling. In contrast, the HGP method can be generalized without increasing the underlying complexity of the algorithm; here we present an implementation of this approach for the first time. A generalized Rys quadrature has been explored previously, however its use was limited to low field strengths owing to the fact that the required quadrature roots and weights were being approximated by a 2D interpolation scheme. Whilst adequate for this purpose, the application of this approach to arbitrary field strengths is problematic as it would necessitate the storage of very large interpolation grids. In addition, it was noted in Ref. 8 that high-precision arithmetic was necessary to determine the required parameters. In this work, we generalize the Rys quadrature approach to a much wider range of field strengths using the approach put forward by Flocke[27] to compute the roots and weights when required.

We commence in Section 2 by discussing some preliminaries, including the use of shell-pair quantities and the transformation between Cartesian and spherical harmonic Gaussians. In Section 3, we discuss the calculation of the one-electron integrals required for practical calculations, including the generalization of the kinetic energy integrals associated with the introduction of a vector potential describing the magnetic field. In Section 4 we describe three approaches to the calculation LAO-ERIs, comparing their relative algorithmic complexity. In Section 5, relative timings for each approach are discussed, illustrating the relative advantages and disadvantages of each algorithm. A mixed scheme, which selects the most efficient algorithm for each class of integral extemporaneously is presented. This mixed approach provides an an effective approach to minimizing the computational cost of the LAO-ERI evaluation.

2 Preliminaries and shell–pair data

In this work we are concerned with the evaluation of molecular integrals over Gaussian–type LAOs. A standard unnormalized Gaussian–type orbital (GTO) has the general form

$$\phi_a(\mathbf{r}) = (x - \mathrm{A}_x)^{a_x} (y - \mathrm{A}_y)^{a_y} (z - \mathrm{A}_z)^{a_z} \sum_{k=1}^{K_a} d_k e^{-\alpha_k |\mathbf{r}-\mathbf{A}|^2} \quad (1)$$

where the function is centred at $\mathbf{A} = (\mathrm{A}_x, \mathrm{A}_y, \mathrm{A}_z)$, has angular momentum $\mathbf{a} = (a_x, a_y, a_z)$ and has exponents $\{\alpha_k\}$ with respective contraction coefficient $\{d_k\}$. Where the contraction length K_a is equal to 1, the GTO only has one exponent with a corresponding contraction coefficient of 1.0 and is a *primitive* GTO, whereas if $K_a > 1$ the GTO is *contracted*. Gaussian–type LAOs are similar to standard GTOs, differing by a phase factor

$$\omega_a(\mathbf{r}) = \phi_a(\mathbf{r}) e^{-i\mathbf{k}_a \cdot \mathbf{r}} \quad (2)$$

where $\mathbf{k}_a$ is the wave vector of the London plane wave, $\mathbf{k}_a = \frac{1}{2}\mathcal{B} \times (\mathbf{A} - \mathbf{O})$, depending on the

external magnetic field $\mathcal{B}$ and relative to the gauge–origin $\mathbf{O}$.

In contemporary molecular integral codes, integrals are almost always computed in shell–batches rather than individually;[28] a shell comprises all basis functions with common centre, exponent and total angular momentum $L_a = a_x + a_y + a_z$ but with different distributions between the three Cartesian components. It is highly advantageous to compute integrals in shell–batches as integrals between individual GTOs within the shells have many common intermediates which may be re–used for all integrals in the batch.

Prior to the calculation of any molecular integrals, the important task of computing shell–pair quantities is carried–out. This serves two main purposes: firstly to streamline subsequent integral evaluation by having key quantities precomputed, reducing their cost from $\mathcal{O}(n^4)$ in the two–electron integrals to $\mathcal{O}(n^2)$ and secondly, to reduce the number of integrals to be calculated by discarding negligible shell–pairs. As each shell–pair describes one charge distribution (i.e. it is simply the product of two shells), if the overlap between the two shells is negligible, it may be discarded. This is particularly important for larger systems, as the number of significant shell–pairs scales only *linearly* with molecule size.[28]

In the evaluation of integrals over LAOs, the computation of shell–pair data can be of further advantage, as the field–related terms can be sequestered within the standard pair quantities, allowing all subsequent integrals (with the exception of kinetic–energy integrals) to be evaluated *without* explicit reference to the complex phase factor.

2.1 Shell–Pairs

In order to discuss the relevance of shell–pairs, it is first necessary to define the charge distributions comprised of products of LAOs,

$$\omega_a^*(\mathbf{r})\omega_b(\mathbf{r}) = \sum_{\mu=1}^{K_a}\sum_{\nu=1}^{K_b}[\mathbf{a}_\mu\mathbf{b}_\nu| = (\mathbf{ab}| \qquad (3)$$

where the notation $[\mathbf{a}_\mu\mathbf{b}_\nu|$ represents the product of the μ^{th} and ν^{th} individual contractions of ω_a and ω_b respectively, whilst $(\mathbf{ab}|$ is the overall inner product of the two LAOs; if both are primitive, the two definitions are equivalent. As will be discussed in the following sections, algorithms for the computation of molecular integrals contain steps that may only be applied to primitive functions, hence shell–pair quantities are calculated for each $[\mathbf{a}_\mu\mathbf{b}_\nu|$ in the charge distribution.

Given an individual pair of primitive functions, centred on $\mathbf{A}$ and $\mathbf{B}$, with exponents α and β and contraction coefficients d_a and d_b respectively, the following pairwise quantities are computed

$$\begin{aligned} \zeta &= \alpha + \beta \qquad & \mathbf{P} &= \frac{1}{\zeta}\left(\alpha\mathbf{A} + \beta\mathbf{B}\right) \\ U_\mathrm{P} &= d_\mathrm{a}d_\mathrm{b}\left(\frac{\pi}{\zeta}\right)^{\frac{3}{2}}\exp\left(-\frac{\alpha\beta}{\zeta}\left|\mathbf{A}-\mathbf{B}\right|^2\right) \end{aligned} \qquad (4)$$

To account for the complex phase factor, the following additional pairwise quantities are evaluated

$$\begin{aligned} \boldsymbol{\chi}_\mathrm{P} &= \frac{1}{2}\mathcal{B}\times(\mathbf{B}-\mathbf{A}) \\ \mathcal{K}_\mathrm{P} &= \exp\left(-\frac{1}{4\zeta}\boldsymbol{\chi}_\mathrm{P}\cdot\boldsymbol{\chi}_\mathrm{P} - i\mathbf{P}\cdot\boldsymbol{\chi}_\mathrm{P}\right) \end{aligned} \qquad (5)$$

Hence for each primitive pair, the pertinent quantities to be stored are simply

$$2\alpha, \quad 2\beta, \quad \frac{1}{2\zeta}, \quad \tilde{\mathbf{P}} = \mathbf{P} - \frac{i}{2\zeta}\boldsymbol{\chi}_\mathrm{P}, \quad \tilde{U}_\mathrm{P} = U_\mathrm{P}\mathcal{K}_\mathrm{P}. \qquad (6)$$

However, if $\left|\tilde{U}_\mathrm{P}\right| \leqslant 10^{-12}$ the pair is considered negligible and discarded from the shell–pair; this allows an increasingly large proportion of the Gaussian product space to be discarded as the system becomes larger. Within this framework of (reduced) shell–pairs, the contraction of Eq. (3) may be applied as early as possible in each integral algorithm to yield contracted integrals.

Advocates of the shell–pair approach have noted that the number of components within a charge distribution may be minimized by a process of modelling the shell–pair with as few

primitive components as possible but which yields a matching electrostatic potential;[28,29] this could yield further efficiencies and may be considered in future work.

2.2 Transformation Matrices

In the computation of ERIs in particular, the horizontal recursion relation (HRR) of Head–Gordon and Pople (HGP),[30] equivalent to the transfer relation of Rys and co-workers,[31] can be used for more efficient treatment of contracted basis functions,

$$(\mathbf{ab} + \mathbf{1}_i| = (\mathbf{a} + \mathbf{1}_i\mathbf{b}| + \mathbf{AB}_i\,(\mathbf{ab}| \qquad (7)$$

This recursion relation, whilst being relatively simple, can grow significantly in cost when the total angular momentum of the integral becomes large.[32,33] Given that this relation is only a two–index quantity, it is convenient to reformulate it as the application of a transformation matrix,[34] allowing the recursion to be efficiently executed as a matrix multiplication,

$$\begin{aligned}(\mathbf{ab}| = &\sum_{e_x=a_x}^{a_x+b_x} \binom{b_x}{e_x} (\mathrm{A}_x - \mathrm{B}_x)^{b_x-e_x} \\ &\times \sum_{e_y=a_y}^{a_y+b_y} \binom{b_y}{e_y} (\mathrm{A}_y - \mathrm{B}_y)^{b_y-e_y} \\ &\times \sum_{e_z=a_z}^{a_z+b_z} \binom{b_z}{e_z} (\mathrm{A}_z - \mathrm{B}_z)^{b_z-e_z}\ (\mathbf{e0}|\,.\end{aligned} \qquad (8)$$

These relatively expensive matrices may be precomputed for each contracted shell–pair and stored along with the quantities in Eq. (6), providing an efficient way of executing the HRR of Eq. (7).

Additionally, if a spherical harmonic Gaussian basis is being used, the Cartesian to spherical transformation can be built into the HRR transformation matrices, eliminating the need for a costly four–index transformation on each shell–quartet and also reducing the size of the HRR matrices to be stored. For standard GTOs, the Cartesian to spherical transformation is that derived by Schlegel and Frisch,[35]

$$\begin{aligned}\mathcal{C}^{\ell m}_{l_x l_y l_z} = &\sqrt{\frac{(2l_x)!(2l_y)!(2l_z)!\ell!(\ell-|m|)!}{(2\ell)!l_x!l_y!l_z!(\ell+|m|)!}}\frac{1}{2^\ell \ell!} \\ &\times \sum_{i=0}^{(\ell-|m|)/2} \binom{\ell}{i}\binom{i}{j}\frac{(-1)^i(2\ell-2i)!}{(\ell-|m|-2i)!} \\ &\times \sum_{k=0}^{j} \binom{j}{k}\binom{|m|}{l_x-2k}(-1)^{\mathrm{sgn}(m)(|m|-l_x+2k)/2}\end{aligned} \qquad (9)$$

in which $\ell = l_x+l_y+l_z$ and $j = (l_x+l_y-|m|)/2$; if j has a half–integer value, the respective $\mathcal{C}^{\ell m}_{l_x l_y l_z} = 0$. Given that the complex component of London orbitals is simply a phase–factor to the real Gaussian–type orbital, the transformation from Cartesian to spherical Gaussian basis is unchanged from the standard case. The transformations for $m = 0$ are real, whilst for nonzero m the complex transformations may be combined into two real forms, $(\mathcal{C}^{\ell m}+\mathcal{C}^{\ell -m})/\sqrt{2}$ for $m > 0$ and $(\mathcal{C}^{\ell m}-\mathcal{C}^{\ell -m})/\sqrt{-2}$ for $m < 0$.

3 One–Electron Integrals

Having assembled the shell–pair quantities, it is necessary to compute the one–electron integrals required for the construction of the Fock matrix; these are the overlap, kinetic energy and nuclear–attraction integrals.

3.1 Overlap Integrals

The two–centre overlap integral is the simplest to compute and is defined for LAOs as

$$(\mathbf{a}\,\mathbf{b}) = \int \omega^*_a(\mathbf{r})\omega_b(\mathbf{r})\mathrm{d}\mathbf{r} \qquad (10)$$

Overlap integrals between Cartesian Gaussian functions are easily computed from shell–pair data using recurrence relations derived by Obara and Saika (OS) from the differential properties of Gaussian functions.[15,36] Given the definitions

$$\mathbf{PA} = \tilde{\mathbf{P}} - \mathbf{A} \qquad [\mathbf{0}\,\mathbf{0}] = \tilde{U}_\mathrm{P} \qquad (11)$$

and the separability of the integrand by Cartesian axes, overlap integrals of higher angular momentum can be obtained by applying the re-

cursion relation to primitive integrals in each Cartesian axis

$$[\mathbf{a}+\mathbf{1}_i\,\mathbf{b}] = \mathbf{PA}_i\,[\mathbf{a}\,\mathbf{b}] + \frac{a_i}{2\zeta}\,[\mathbf{a}-\mathbf{1}_i\,\mathbf{b}] + \frac{b_i}{2\zeta}\,[\mathbf{a}\,\mathbf{b}-\mathbf{1}_i] \quad (12)$$

A primitive overlap integral may then be computed as

$$[\mathbf{a}\,\mathbf{b}] = [a_x\,b_x]\cdot[a_y\,b_y]\cdot[a_z\,b_z] \quad (13)$$

which is then contracted according to Eq. (3) and transformed into a spherical Gaussian basis if required.

3.2 Multipole, Differential and Kinetic Energy Integrals

The kinetic energy integrals are slightly more complicated to evaluate than overlap integrals due to the presence of the diamagnetic and paramagnetic terms in the kinetic energy operator, which are not normally considered in the zero–field case. In the Coulomb gauge, the kinetic energy operator is given by half the square of the kinetic–momentum operator $\hat{\pi}$, thus the kinetic energy integral is defined as

$$\left(\mathbf{a}\left|\frac{1}{2}\hat{\pi}^2\right|\mathbf{b}\right) = \frac{1}{2}\int \omega_a^*(\mathbf{r})\hat{\pi}^2\omega_b(\mathbf{r})\mathrm{d}\mathbf{r}. \quad (14)$$

In a uniform field $\mathcal{B}$, the square of the kinetic–momentum operator at position $\mathbf{R}$ can be expanded as

$$\begin{aligned}\hat{\pi}^2 &= \left(-i\nabla + \frac{1}{2}\mathcal{B}\times\mathbf{R}\right)^2 \\ &= -\nabla^2 - \frac{i}{2}\nabla\,(\mathcal{B}\times\mathbf{R}) - \frac{i}{2}\,(\mathcal{B}\times\mathbf{R})\,\nabla + \frac{1}{4}\,(\mathcal{B}\times\mathbf{R})^2\end{aligned} \quad (15)$$

Considering the x–component of this operator, Eq. (15) may be further resolved by substituting the corresponding components for the cross–products,

$$\begin{aligned}\hat{\pi}_x^2 = &-\frac{\partial^2}{\partial x^2} - \frac{i}{2}\frac{\partial}{\partial x}\,(\mathcal{B}_y\mathbf{R}_z - \mathcal{B}_z\mathbf{R}_y) \\ &- \frac{i}{2}\,(\mathcal{B}_y\mathbf{R}_z - \mathcal{B}_z\mathbf{R}_y)\,\frac{\partial}{\partial x} + \frac{1}{4}\,(\mathcal{B}_y\mathbf{R}_z - \mathcal{B}_z\mathbf{R}_y)^2\end{aligned} \quad (16)$$

Given that the total kinetic energy operator is equal to

$$\frac{1}{2}\hat{\pi}^2 = \frac{1}{2}\hat{\pi}_x^2 + \frac{1}{2}\hat{\pi}_y^2 + \frac{1}{2}\hat{\pi}_z^2, \quad (17)$$

the integral is separable into the sum of its components in each of the Cartesian directions and it can be evaluated as such; the operator for the x–component is given by

$$\begin{aligned}\frac{1}{2}\hat{\pi}_x^2 = &-\frac{1}{2}\frac{\partial^2}{\partial x^2} - \frac{i}{2}\mathcal{B}_y\frac{\partial}{\partial x}\mathbf{R}_z + \frac{i}{2}\mathcal{B}_z\frac{\partial}{\partial x}\mathbf{R}_y \\ &+ \frac{1}{8}\mathcal{B}_y^2\mathbf{R}_z^2 + \frac{1}{8}\mathcal{B}_z^2\mathbf{R}_y^2 - \frac{1}{4}\mathcal{B}_y\mathcal{B}_z\mathbf{R}_y\mathbf{R}_z,\end{aligned} \quad (18)$$

with equivalent expressions defining the y and z components. All required terms are derived from the corresponding overlap integrals, computed in the standard way described in subsection 3.1. From these, multipole and differential integrals up to second order are obtained by application of their respective recursion relations. For simplicity of notation, n^{th}–order multipole and differential operators are respectively denoted as

$$(x-O_x)^n \rightarrow x_o^n \qquad \frac{\partial^n}{\partial x^n} \rightarrow \partial_x^n \quad (19)$$

This leads to the following relation for multipole operators,

$$\left[\mathbf{a}\left|x_o^{n+1}\right|\mathbf{b}\right] = \mathbf{BO}_x\,[\mathbf{a}\,|x_o^n|\,\mathbf{b}] + [\mathbf{a}\,|x_o^n|\,\mathbf{b}+\mathbf{1}_x] \quad (20)$$

and the corresponding recursion relation for differential operators,

$$\begin{aligned}\left[\mathbf{a}\left|\partial_x^{n+1}\right|\mathbf{b}\right] = &\; b_x\,[\mathbf{a}\,|\partial_x^n|\,\mathbf{b}-\mathbf{1}_x] - i\mathbf{k}_{b,x}\,[\mathbf{a}\,|\partial_x^n|\,\mathbf{b}] \\ &- 2\beta\,[\mathbf{a}\,|\partial_x^n|\,\mathbf{b}+\mathbf{1}_x]\end{aligned} \quad (21)$$

where $\mathbf{O}$ is the gauge–origin, $\mathbf{k}_b$ the London phase–factor at $\mathbf{B}$, and

$$\left[\mathbf{a}\left|x_o^0\right|\mathbf{b}\right] = \left[\mathbf{a}\left|\partial_x^0\right|\mathbf{b}\right] = [\mathbf{a}\,\mathbf{b}] \quad (22)$$

Higher order multipole and differential integrals can be obtained by repeated application of the above recurrence relations. The final expression for the x–component of the kinetic energy

integral is given by

$$\begin{aligned}\left[\mathbf{a}\left|\frac{1}{2}\hat{\pi}_x^2\right|\mathbf{b}\right] =& -\frac{1}{2}\left[a_x\middle|\partial_x^2\middle|b_x\right]\cdot[a_y\,b_y]\cdot[a_z\,b_z]\\ &+\frac{i}{2}\mathcal{B}_z\left[a_x\middle|\partial_x\middle|b_x\right]\cdot[a_y\,|y_o|\,b_y]\cdot[a_z\,b_z]\\ &-\frac{i}{2}\mathcal{B}_y\left[a_x\middle|\partial_x\middle|b_x\right]\cdot[a_y\,b_y]\cdot[a_z\,|z_o|\,b_z]\\ &+\frac{1}{8}\mathcal{B}_y^2\left[a_x\,b_x\right]\cdot[a_y\,b_y]\cdot\left[a_z\left|z_o^2\right|b_z\right]\\ &+\frac{1}{8}\mathcal{B}_z^2\left[a_x\,b_x\right]\cdot\left[a_y\left|y_o^2\right|b_y\right]\cdot[a_z\,b_z]\\ &-\frac{1}{4}\mathcal{B}_y\mathcal{B}_z\left[a_x\,b_x\right]\cdot[a_y\,|y_o|\,b_y]\cdot[a_z\,|z_o|\,b_z],\end{aligned} \tag{23}$$

with equivalent expressions for the y and z–components. Hence from Eq. (17), the primitive kinetic energy integral is given by

$$\left[\mathbf{a}\left|\frac{1}{2}\hat{\pi}^2\right|\mathbf{b}\right] = \left[\mathbf{a}\left|\frac{1}{2}\hat{\pi}_x^2\right|\mathbf{b}\right] + \left[\mathbf{a}\left|\frac{1}{2}\hat{\pi}_y^2\right|\mathbf{b}\right] + \left[\mathbf{a}\left|\frac{1}{2}\hat{\pi}_z^2\right|\mathbf{b}\right]. \tag{24}$$

In the same way as for the overlap integrals, kinetic–energy integrals over LAOs are computed in the primitive Cartesian Gaussian basis for a given shell–pair, and subsequently contracted according to Eq. (3) and transformed into the spherical Gaussian basis if required.

3.3 Nuclear Attraction Integrals

In contrast to the aforementioned one–electron integrals, the nuclear attraction integral is not separable into Cartesian components due to the Coulomb operator that defines the integral,

$$\left(\mathbf{a}\left|\frac{1}{\mathbf{r}_C}\right|\mathbf{b}\right) = \int \frac{\omega_a^*(\mathbf{r})\omega_b(\mathbf{r})}{|\mathbf{r}-\mathbf{C}|}\mathrm{d}\mathbf{r}, \tag{25}$$

where $\mathbf{C}$ is the position of an atomic nucleus with unit charge. The most common approach to computing such integrals is to reduce them by applying the Gaussian product theorem and substituting the Coulomb operator with its Laplace transform

$$\frac{1}{\mathbf{r}} = \frac{2}{\sqrt{\pi}}\int_0^\infty \exp(-u^2|\mathbf{r}|^2)\mathrm{d}u, \tag{26}$$

to yield a one–dimensional integral that can be approximated numerically relatively inexpensively, using the molecular incomplete gamma function. The derivation of this transformation is extensively detailed in the literature, for example in Refs. 28,37,38.

The molecular incomplete gamma function, also known as the Boys Function, is formally defined as[39]

$$\mathsf{F}_\mathrm{m}(z) = \int_0^1 t^{2\mathrm{m}}\exp(-zt^2)\mathrm{d}t, \tag{27}$$

thus is a transcendental function related to the error function `erf` by

$$\mathsf{F}_0(z) = \sqrt{\frac{\pi}{4z}}\mathrm{erf}\left(\sqrt{z}\right) \tag{28}$$

and identified as a scaled form of Kummer's confluent hypergeometric function $M(a,b,z)$,[40]

$$\mathsf{F}_\mathrm{m}(z) = \frac{1}{2\mathrm{m}+1}M\left(\mathrm{m}+\frac{1}{2},\mathrm{m}+\frac{3}{2},-z\right) \quad m > -\frac{1}{2}. \tag{29}$$

Differentiation of the Boys Function with respect to the argument yields

$$\frac{\mathrm{d}}{\mathrm{d}z}\mathsf{F}_\mathrm{m}(z) = -\mathsf{F}_{\mathrm{m}+1}(z), \tag{30}$$

from which the following recurrence relation can be derived using integration by parts,

$$\begin{aligned}\mathsf{F}_\mathrm{m}(z) &= \left[\frac{t^{2\mathrm{m}+1}}{2\mathrm{m}+1}\exp(-zt^2)\right]_{t=0}^{t=1} - \int_0^1 \frac{-2zt^{2\mathrm{m}+2}}{2\mathrm{m}+1}\exp(-zt^2)\mathrm{d}t\\ &= \frac{1}{2\mathrm{m}+1}\left\{\exp(-z) + 2z\int_0^1 t^{2(\mathrm{m}+1)}\exp(-zt^2)\mathrm{d}t\right\}\\ &= \frac{1}{2\mathrm{m}+1}\left\{\exp(-z) + 2z\mathsf{F}_{\mathrm{m}+1}(z)\right\}.\end{aligned} \tag{31}$$

Repeated application of this recursion relation yields a series expansion that may be used to approximate the Boys Function[37]

$$\mathsf{F}_\mathrm{m}(z) = \exp(-z)\sum_{i=0}^{\infty}\frac{(2\mathrm{m}-1)!!(2z)^i}{(2\mathrm{m}+2i+1)!!}. \tag{32}$$

The expansion in Eq. (32) provides a numerically stable means of approximating $\mathsf{F}_\mathrm{m}(z)$ for a relatively wide range of arguments, z. However, the series converges rapidly and thus the approximation is most suited for smaller arguments $|z| \leqslant 25.0$. At larger z, corresponding to well–separated shell pairs that are increasingly prevalent in large systems, the Boys Function may be efficiently computed by the much sim-

pler asymptotic approximation,

$$\mathsf{F}_{\mathrm{m}}(z) \approx \frac{(2\mathrm{m}-1)!!}{2^{\mathrm{m}+1}}\sqrt{\frac{\pi}{z^{2\mathrm{m}+1}}}. \qquad (33)$$

For convenience, the following intermediate function is defined that combines the Boys Function with a pre–factor by which it is always multiplied

$$\mathsf{G}_{\mathrm{m}}(z) = \sqrt{\frac{2}{\pi}}\mathsf{F}_{\mathrm{m}}(z) \qquad (34)$$

The principle difference in approximating the Boys Function for integrals over LAOs as rather than standard GTOs is that the argument z is generally complex with LAOs, whilst it is always real with GTOs. With a complex argument, the standard methods of approximation may be less stable numerically and become unreliable, thus a careful approach is required. This problem has been extensively studied in Refs. 41–43 and a multitude of methods examined for different ranges of z.

In the present work, Eqs. (32) and (33) have been tested along with several from Ref. 42 against a range of complex argument z. There were no difficulties with numerical instability observed in the implementation of Eqs. (32) and (33) and no improvement was observed by using alternative methods. At present, a combination of Eqs. (32) and (33) appear sufficient to provide a reliable method of approximating the Boys Function for complex argument.

With a stable method of approximating the Boys Function available, shell–pair data makes it simple to generalise the OS recursion relation for nuclear attraction integrals over GTOs[15] to those over LAOs. The OS recursion relation requires a set of auxiliary integrals, derived in detail in Ref. 15, to enable the incrementation of angular momentum for each function. For each primitive integral, the shell–pair data and nuclear position are used to calculate the parameters,

$$\mathbf{PC} = \tilde{\mathbf{P}} - \mathbf{C} \qquad R^2 = |\mathbf{PC}|^2 \qquad Z_{\mathrm{PC}} = \zeta R^2, \quad (35)$$

from which the auxiliary integrals are be constructed as

$$\left[\mathbf{0}\left|\frac{1}{\mathbf{r}_C}\right|\mathbf{0}\right]^{(\mathrm{m})} = \begin{cases} \tilde{U}_{\mathrm{P}}\,(2\zeta)^{\mathrm{m}+\frac{1}{2}}\,\mathsf{G}_{\mathrm{m}}\,(Z_{\mathrm{PC}}) & |Z_{\mathrm{PC}}| \leqslant 25.0 \\ \tilde{U}_{\mathrm{P}}\frac{(2\mathrm{m}-1)!!}{R^{2\mathrm{m}+1}} & |Z_{\mathrm{PC}}| > 25.0 \end{cases} \qquad (36)$$

The OS recursion relation for the nuclear attraction integral has the form

$$\begin{aligned}
\left[\mathbf{a}+\mathbf{1}_i\left|\frac{1}{\mathbf{r}_C}\right|\mathbf{b}\right]^{(\mathrm{m})} &= \mathbf{PA}_i\left[\mathbf{a}\left|\frac{1}{\mathbf{r}_C}\right|\mathbf{b}\right]^{(\mathrm{m})} - \mathbf{PC}_i\left(\frac{1}{2\zeta}\right)\left[\mathbf{a}\left|\frac{1}{\mathbf{r}_C}\right|\mathbf{b}\right]^{(\mathrm{m}+1)} \\
&+ a_i\left(\frac{1}{2\zeta}\right)\left\{\left[\mathbf{a}-\mathbf{1}_i\left|\frac{1}{\mathbf{r}_C}\right|\mathbf{b}\right]^{(\mathrm{m})} - \left(\frac{1}{2\zeta}\right)\left[\mathbf{a}-\mathbf{1}_i\left|\frac{1}{\mathbf{r}_C}\right|\mathbf{b}\right]^{(\mathrm{m}+1)}\right\} \\
&+ b_i\left(\frac{1}{2\zeta}\right)\left\{\left[\mathbf{a}\left|\frac{1}{\mathbf{r}_C}\right|\mathbf{b}-\mathbf{1}_i\right]^{(\mathrm{m})} - \left(\frac{1}{2\zeta}\right)\left[\mathbf{a}\left|\frac{1}{\mathbf{r}_C}\right|\mathbf{b}-\mathbf{1}_i\right]^{(\mathrm{m}+1)}\right\} \\
\left[\mathbf{a}\left|\frac{1}{\mathbf{r}_C}\right|\mathbf{b}+\mathbf{1}_i\right]^{(\mathrm{m})} &= \mathbf{PB}_i\left[\mathbf{a}\left|\frac{1}{\mathbf{r}_C}\right|\mathbf{b}\right]^{(\mathrm{m})} - \mathbf{PC}_i\left(\frac{1}{2\zeta}\right)\left[\mathbf{a}\left|\frac{1}{\mathbf{r}_C}\right|\mathbf{b}\right]^{(\mathrm{m}+1)} \\
&+ a_i\left(\frac{1}{2\zeta}\right)\left\{\left[\mathbf{a}-\mathbf{1}_i\left|\frac{1}{\mathbf{r}_C}\right|\mathbf{b}\right]^{(\mathrm{m})} - \left(\frac{1}{2\zeta}\right)\left[\mathbf{a}-\mathbf{1}_i\left|\frac{1}{\mathbf{r}_C}\right|\mathbf{b}\right]^{(\mathrm{m}+1)}\right\} \\
&+ b_i\left(\frac{1}{2\zeta}\right)\left\{\left[\mathbf{a}\left|\frac{1}{\mathbf{r}_C}\right|\mathbf{b}-\mathbf{1}_i\right]^{(\mathrm{m})} - \left(\frac{1}{2\zeta}\right)\left[\mathbf{a}\left|\frac{1}{\mathbf{r}_C}\right|\mathbf{b}-\mathbf{1}_i\right]^{(\mathrm{m}+1)}\right\}
\end{aligned} \qquad (37)$$

where the superscript index m denotes an m^{th}–order auxiliary integral; final integrals have $\mathrm{m} = 0$. Once these have been computed in the primitive Cartesian Gaussian basis for each shell–pair and nucleus, the integral batch is contracted according to Eq. (3) and transformed into the spherical Gaussian basis if necessary.

4 Two–Electron Integrals

The two–electron integrals present a much greater computational task than do the one–electron integrals; they are both individually more complex to evaluate than, and outnumber by orders of magnitude, their one–electron counterparts. In addition, ERIs over LAOs have a lower order of permutational symmetry than those over standard GTOs, with twice as many needing to be computed. Their efficient evaluation is therefore of much importance. We consider LAO–ERIs of the form

$$(\mathbf{ab}|\mathbf{cd}) = \iint \frac{\omega_a^*(\mathbf{r}_1)\omega_b(\mathbf{r}_1)\omega_c^*(\mathbf{r}_2)\omega_d(\mathbf{r}_2)}{|\mathbf{r}_1-\mathbf{r}_2|}\mathrm{d}\mathbf{r}_1\mathrm{d}\mathbf{r}_2, \quad (38)$$

where the presence of the Coulomb operator again requires a transformation similar to that for nuclear attraction integrals, detailed in the literature.[28,37,38] A common approach is to introduce the molecular incomplete gamma function and construct a set of auxiliary intermediates, analogous to that described in subsection 3.3, then apply recursion relations to gener-

ate the integrals from these auxiliaries. A long–established alternative to this is to generate the *integrands* from unity by recursion and evaluate the integral using a Gaussian quadrature with the Rys weight function,[20,21] discussed in detail in subsection 4.3.

Several algorithms by which these ERIs may be computed are set–out here, each having their own advantages and disadvantages. They do however all require the same set of intermediate quantities for each shell–quartet,[28]

$$\begin{array}{lll} \mathbf{PQ} = \tilde{\mathbf{P}} - \tilde{\mathbf{Q}} & R^2 = |\mathbf{PQ}|^2 & 2\vartheta = \left\{\frac{1}{2\zeta} + \frac{1}{2\eta}\right\}^{-1} \\ U_{\mathrm{PQ}} = \tilde{U}_{\mathrm{P}}\tilde{U}_{\mathrm{Q}} & Z_{\mathrm{PQ}} = \vartheta R^2 & \end{array} \quad (39)$$

all of which are readily constructed from shell–pair data, where η, $\tilde{U}_{\mathrm{Q}}$ and $\tilde{\mathbf{Q}}$ are the second shell–pair equivalent of ζ, $\tilde{U}_{\mathrm{P}}$ and $\tilde{\mathbf{P}}$ respectively.

4.1 The McMurchie Davidson algorithm

The algorithm that is most established for practical use in calculating ERIs over LAOs is the MD algorithm,[22] in which charge distributions are expanded in Hermite Gaussian functions. Integrals are then computed over the Hermite Gaussian functions and transformed back into the Cartesian basis.

This approach is effective in the absence of an external field, as the use of Hermite functions allows the four centre integral to be reduced to just one centre, resulting in a recurrence relation for incrementing angular momentum of only two terms. The result of this is that the recursion step in the MD algorithm becomes more advantageous with higher total angular momentum, however the MD algorithm is disadvantaged by the substantial computational cost of transforming the Hermite integrals back to the Cartesian basis.

The expansion of AOs with a complex phase factor in a Hermite Gaussian basis has been the most widely practised approach to evaluation of the necessary integrals; Colle *et. al.* presented general formulae for integrals over Hermite Gaussian functions with complex phase factors in Refs. 44,45, noting that transforming the integrals to the Cartesian basis would be a trivial extension. Further progress has been made by Tachikawa and co–workers[23,24] and by Tellgren *et. al*[1,3] to generalise the MD algorithm for the evaluation of integrals over Gaussian functions with a complex phase–factor.

In the interests of comparison, the generalised MD algorithm was implemented as part of the present study, broadly following the scheme detailed in Ref. 1, but adapted to the context of the shell–pair scheme. The zeroth–order Hermite integrals are computed from the molecular incomplete gamma function as

$$[\mathbf{0}]^{(\mathrm{m})} = \begin{cases} U_{\mathrm{PQ}}(-1)^{\mathrm{m}}\,(2\vartheta)^{\mathrm{m}+\frac{1}{2}}\,\mathsf{G}_{\mathrm{m}}\,(Z_{\mathrm{PQ}}) & |Z_{\mathrm{PQ}}| \leqslant 25.0 \\ U_{\mathrm{PQ}}(-1)^{\mathrm{m}}\frac{(2\mathrm{m}-1)!!}{R^{2\mathrm{m}+1}} & |Z_{\mathrm{PQ}}| > 25.0 \end{cases} \quad (40)$$

from which two–centre Hermite integrals of higher angular momentum are calculated recursively as

$$\begin{aligned} [\mathbf{p}+\mathbf{1}_i|\mathbf{q}]^{(\mathrm{m})} &= -i\boldsymbol{\chi}_{\mathrm{P},i}\,[\mathbf{p}|\mathbf{q}]^{(\mathrm{m})} + \mathbf{PQ}_i\,[\mathbf{p}|\mathbf{q}]^{(\mathrm{m}+1)} \\ &\quad + p_i\,[\mathbf{p}-\mathbf{1}_i|\mathbf{q}]^{(\mathrm{m}+1)} - q_i\,[\mathbf{p}|\mathbf{q}-\mathbf{1}_i]^{(\mathrm{m}+1)} \\ [\mathbf{p}|\mathbf{q}+\mathbf{1}_i]^{(\mathrm{m})} &= -i\boldsymbol{\chi}_{\mathrm{Q},i}\,[\mathbf{p}|\mathbf{q}]^{(\mathrm{m})} - \mathbf{PQ}_i\,[\mathbf{p}|\mathbf{q}]^{(\mathrm{m}+1)} \\ &\quad - p_i\,[\mathbf{p}-\mathbf{1}_i|\mathbf{q}]^{(\mathrm{m}+1)} + q_i\,[\mathbf{p}|\mathbf{q}-\mathbf{1}_i]^{(\mathrm{m}+1)} \end{aligned} \quad (41)$$

When considering non–zero external field, a consequence of the complex phase factor in LAOs is that the four centre integral can no longer be simplified to a one centre integral over Hermite Gaussian functions; instead it can only be reduced to a two centre integral, with the recursion relation used to increment angular momentum comprising double the number of terms.[1] Thus the principle advantage of this algorithm is lost, whilst the costly transformation from Hermite to Cartesian Gaussians remains necessary and is given by

$$\begin{aligned} [\mathbf{a}+\mathbf{1}_i\,\mathbf{b}\,\mathbf{p}| &= p_i\,[\mathbf{a}\,\mathbf{b}\,\mathbf{p}-\mathbf{1}_i| + \mathbf{PA}_i\,[\mathbf{a}\,\mathbf{b}\,\mathbf{p}| + \left(\frac{1}{2\zeta}\right)[\mathbf{a}\,\mathbf{b}\,\mathbf{p}+\mathbf{1}_i| \\ |\mathbf{q}\,\mathbf{c}+\mathbf{1}_i\,\mathbf{d}] &= q_i\,|\mathbf{q}-\mathbf{1}_i\,\mathbf{c}\,\mathbf{d}] + \mathbf{QC}_i\,|\mathbf{q}\,\mathbf{c}\,\mathbf{d}] + \left(\frac{1}{2\eta}\right)|\mathbf{q}+\mathbf{1}_i\,\mathbf{c}\,\mathbf{d}]\,. \end{aligned} \quad (42)$$

These transformations are unchanged from those in the zero–field algorithm, allowing any techniques developed to optimise this step to be applied to integrals over LAOs. In particular, the Hermite to Cartesian recursion of Eq. (42) and the contraction stage of Eq. (3) be applied

to one index of the Hermite integral at a time, improving efficiency as Eq. (42) can then be applied to the other index with the integral already half contracted.

4.2 The Head–Gordon Pople algorithm

In view of the apparent shortcomings of the MD algorithm when applied to integrals over LAOs, this work has sought to identify and implement alternative methods that will allow the integrals to be computed with greater efficiency.

The first of these to be considered is an adaptation of the HGP algorithm, itself a modification of the OS scheme.[28,30] In this approach, the zeroth–order auxiliary integrals are constructed in much the same way as for the nuclear attraction integrals, from the molecular incomplete gamma function scaled with the requisite pre–factors

$$[\mathbf{0}]^{(\mathrm{m})} = \begin{cases} U_{\mathrm{PQ}} \left(2\vartheta\right)^{\mathrm{m}+\frac{1}{2}} \mathsf{G}_{\mathrm{m}}\left(Z_{\mathrm{PQ}}\right) & |Z_{\mathrm{PQ}}| \leqslant 25.0 \\ U_{\mathrm{PQ}} \frac{(2\mathrm{m}-1)!!}{R^{2\mathrm{m}+1}} & |Z_{\mathrm{PQ}}| > 25.0 \end{cases} \tag{43}$$

From these auxiliary integrals, angular momentum can be incremented at each of the indices by applying the eight–term OS recursion relation.[15] In the HGP algorithm, this is significantly simplified by building up angular momentum at only two indices, reducing the number of terms present in the recursion relation from eight to five, given by

$$\begin{aligned} [\mathbf{e}+\mathbf{1}_i\mathbf{0}|\mathbf{f0}]^{(\mathrm{m})} &= \mathbf{PA}_i\,[\mathbf{e0}|\mathbf{f0}]^{(\mathrm{m})} - \mathbf{PQ}_i\left(\frac{1}{2\zeta}\right)[\mathbf{e0}|\mathbf{f0}]^{(\mathrm{m}+1)} \\ &\quad + e_i\left(\frac{1}{2\zeta}\right)\left\{[\mathbf{e}-\mathbf{1}_i\mathbf{0}|\mathbf{f0}]^{(\mathrm{m})} - \left(\frac{1}{2\zeta}\right)[\mathbf{e}-\mathbf{1}_i\mathbf{0}|\mathbf{f0}]^{(\mathrm{m}+1)}\right\} \\ &\quad + f_i\left(\frac{1}{2\zeta}\right)\left(\frac{1}{2\eta}\right)[\mathbf{e0}|\mathbf{f}-\mathbf{1}_i\mathbf{0}]^{(\mathrm{m}+1)} \\ [\mathbf{e0}|\mathbf{f}+\mathbf{1}_i\mathbf{0}]^{(\mathrm{m})} &= \mathbf{QC}_i\,[\mathbf{e0}|\mathbf{f0}]^{(\mathrm{m})} + \mathbf{PQ}_i\left(\frac{1}{2\eta}\right)[\mathbf{e0}|\mathbf{f0}]^{(\mathrm{m}+1)} \\ &\quad + f_i\left(\frac{1}{2\eta}\right)\left\{[\mathbf{e0}|\mathbf{f}-\mathbf{1}_i\mathbf{0}]^{(\mathrm{m})} - \left(\frac{1}{2\eta}\right)[\mathbf{e0}|\mathbf{f}-\mathbf{1}_i\mathbf{0}]^{(\mathrm{m}+1)}\right\} \\ &\quad + e_i\left(\frac{1}{2\eta}\right)\left(\frac{1}{2\zeta}\right)[\mathbf{e}-\mathbf{1}_i\mathbf{0}|\mathbf{f0}]^{(\mathrm{m}+1)} \end{aligned} \tag{44}$$

where $L_e = \{L_a, L_a + L_b\}$ and $L_f = \{L_c, L_c + L_d\}$. A further significant advantage of the HGP scheme is that the integrals may be contracted at this stage, before applying the HRR of subsection 2.2, yielding the contracted intermediate

$$(\mathbf{e0}|\mathbf{f0}) = \sum_{K_a}\sum_{K_b}\sum_{K_c}\sum_{K_d}[\mathbf{e0}|\mathbf{f0}]^{(0)}\,. \tag{45}$$

With the pre–computed transformation matrices of Eq. (8), the HRR (in combination with spherical transformation if necessary) may be simply applied as

$$\begin{aligned} (\mathbf{e0}|\mathbf{cd}) &= \sum_{\mathbf{f}}(\mathbf{e0}|\mathbf{f0})\,(\mathbf{f}|\mathbf{cd}) \\ (\mathbf{ab}|\mathbf{cd}) &= \sum_{\mathbf{e}}(\mathbf{ab}|\mathbf{e})\,(\mathbf{e0}|\mathbf{cd}) \end{aligned} \tag{46}$$

where $(\mathbf{ab}|\mathbf{e})$ and $(\mathbf{f}|\mathbf{cd})$ are the transformation matrices for the each shell–pair respectively, thus providing a significant increase in efficiency when the contraction length of the shell–pairs is high. The matrix multiplication approach to the HRR employed in this work enhances these gains by making use of optimized math libraries.

4.3 The Rys polynomial approach

As a second alternative to the MD scheme, we also consider the generalization of Rys quadrature for the calculation of LAO-ERIs. According to the Gauss quadrature theory, a definite integral of a polynomial $P(x)$ of order up to $2N-1$ weighted by a function $W(x)$ can be computed exactly by summing over N weights w_i multiplied by $P(x)$ evaluated at N roots x_i of a polynomial $p_N(x)$:[27]

$$\int_a^b P(x)W(x)\mathrm{d}x = \sum_{i=1}^{N} P(x_i)w_i. \tag{47}$$

The algorithm to obtain the necessary roots and weights is described in Section 4.3.1. In order to evaluate an ERI using Eq. (47), we have to identify the polynomial and weight function components of its integrand.

Following a Laplace transformation of the Coulomb operator, given in Eq. (26), the in-

tegral can be written as

$$(\mathbf{ab}|\mathbf{cd}) \propto U_{\mathrm{PQ}} \int_0^1 e^{-t^2 Z_{\mathrm{PQ}}} \mathcal{I}_x(t)\mathcal{I}_y(t)\mathcal{I}_z(t)\mathrm{d}t, \quad (48)$$

where $\mathcal{I}_x(t)$, $\mathcal{I}_y(t)$, $\mathcal{I}_z(t)$ are two–dimensional integrals over Cartesian components which depend on the angular momenta and exponents of the quartet. It can be shown that these 2D integrals are polynomials in t^2. Moreover, after a substitution $x = t^2$ we can identify the weight function of Eq. (47) as the exponential part of the integrand in Eq. (48), the so called Rys weight function,[21] $W(x) = e^{-xZ_{\mathrm{PQ}}}/\sqrt{x}$. Hence, the ERI for any shell quartet can be evaluated using the Gauss quadrature technique provided that a set of roots and corresponding weights can be obtained for any value of the argument Z_{PQ}.

In this work, we adapt the algorithm to generate real roots and weights of Golub and Welsh[46] and of Flocke[27] for complex Gauss quadrature needed to compute ERIs over LAOs.

4.3.1 The Gauss Quadrature Rules

For a fixed weight function $W(x) \geqslant 0$ on $x \in [a, b]$, it is possible to define a sequence of real polynomials $p_0(x)$, $p_1(x)$, ..., $p_n(x)$ of the form $p_n(x) = k_n \prod_{j=1}^{n}(x - x_j)$, $k_n > 0$, which are orthogonal with respect to the weight function,

$$\langle p_m(x)|p_n(x)\rangle_w \equiv \int_a^b p_m(x)p_n(x)W(x)\mathrm{d}x = 0, \quad m \neq n. \quad (49)$$

We note that a system of polynomials orthogonal with respect to the Rys weight function are called the Rys polynomials.[20] Any set of real orthogonal polynomials $\{p_n(x)\}_{n=1}^{N}$ can be constructed using a three–term recurrence relation,

$$p_n(x) = (a_n x - b_n)p_{n-1}(x) - c_n p_{n-2}(x) \quad n > 1 \quad (50)$$

where $p_{-1}(x) \equiv 0$ and $p_0(x) \equiv 1$. The two conditions that p_n is orthogonal to p_{n-1} and p_{n-2} do not determine the three coefficients a_n, b_n, and c_n uniquely. Different choices of the third condition are discussed in literature resulting in monic polynomials[27] (the coefficient of the largest power of x is equal to 1) or orthonormal polynomials used in this work and in Ref. 47.

In order to find N roots $\{x_i\}$ of $p_N(x)$ required in Eq. (47), the recurrence relation of Eq. (50) can be written in a matrix form as

$$x\mathbf{p}(x) = T\mathbf{p}(x) + p_N(x)\mathbf{e}_N, \quad (51)$$

where $\mathbf{p}(x) = [p_0(x), p_1(x), \ldots, p_{N-1}(x)]^T$, $\mathbf{e}_N = [0, 0, \ldots, 1]^T$ and T is the tridiagonal matrix

$$T = \begin{bmatrix} b_1/a_1 & 1/a_1 & & & \\ c_2/a_2 & b_2/a_2 & 1/a_2 & & \\ & c_3/a_3 & b_3/a_3 & \ldots & \\ & & \ldots & \ldots & 1/a_{N-1} \\ & & & c_N/b_N & b_N/a_N \end{bmatrix}, \quad (52)$$

which becomes symmetric in case of an orthonormal polynomial set $\{q_n(x)\}_{n=1}^{N}$ with $q_0(x) \equiv (\int_a^b W(x)\mathrm{d}x)^{-1/2}$ chosen to satisfy $\langle q_0(x)|q_0(x)\rangle_w = 1$ (see Refs. 47,48 for a more detailed discussion). A transition to recursion coefficients generating an orthonormal sequence of polynomials corresponds to a similarity transformation to Jacobi matrix $J = DTD^{-1}$, where

$$J = \begin{bmatrix} \alpha_0 & \beta_1 & & & \\ \beta_1 & \alpha_1 & \beta_2 & & \\ & \beta_2 & \alpha_2 & \ldots & \\ & & \ldots & \ldots & \beta_{N-1} \\ & & & \beta_{N-1} & \alpha_{N-1} \end{bmatrix}, \quad (53)$$

where $\alpha_n = b_n/a_n$ and $\beta_n = (-a_n a_{n+1}/c_{n+1})^{-1/2}$.

In analogy to Eq. (51), we can write a matrix equation $x\mathbf{q}(x) = J\mathbf{q}(x) + q_N(x)\mathbf{e}_N$. Solving the characteristic equation $x_i\mathbf{q}(x_i) = J\mathbf{q}(x_i)$ leads to $q_N(x_i) = 0$, hence the eigenvalues of matrix J (and T) are the required roots.

Our matrix J is symmetric and real (i.e., Hermitian) so its set of eigenvectors $\{\mathbf{q}(x_i)\}_{i=1}^{N}$ associated with eigenvalues x_i is orthogonal with respect to the standard inner product

$$\langle \mathbf{q}(x_i)|\mathbf{q}(x_j)\rangle \equiv \sum_{n=1}^{N} \mathbf{q}_n(x_i)\overline{\mathbf{q}_n(x_j)} = 0, \quad i \neq j. \quad (54)$$

However, these eigenvectors are not normalized by virtue of the method with which they are constructed. For the corresponding weights w_i, as a consequence of the Christoffel–Darboux identity we have:[46,48] $w_i \sum_{n=1}^{N} \mathbf{q}_n^2(x_i) = 1$.

We can find a orthonormal set of eigenvectors $\{\mathbf{u}_i\}_{i=1}^N$, forming columns of a unitary matrix U which satisfies the identity $U^\dagger U = E$ in general and $U^T U = E$ in the case of real eigenvectors. The combination of this and the Christoffel–Darboux identity allows us to write an explicit expression for the weights w_i as

$$w_i = \frac{\mathbf{u}_{j,i}^2}{\mathbf{q}_j^2(x_i)} \qquad j = 1, \ldots, N. \tag{55}$$

Finally, we can use the fact that the first component of any eigenvector $\mathbf{q}(x_i)$ is a constant

$$\mathbf{q}_1(x_i) = q_0 \equiv \left(\int_a^b W(x) \mathrm{d}x \right)^{-1/2} \tag{56}$$

and obtain $w_i = u_{1,i}^2 \int_a^b W(x)\mathrm{d}x$. The problem of evaluating the ERIs is now reduced to obtaining the recurrence coefficients a_n, b_n, and c_n.

Unfortunately, the Rys polynomials do not belong to any classical sets of orthogonal polynomials with known recurrence coefficients. Several alternative Rys quadrature methods are reviewed in Ref. 27, highlighting the efficiency and numerical stability of the modified moment method[49] for real positive values of the argument Z_{PQ}. Here we adopt this method for complex values of Z_{PQ}, which occur for integrals over LAOs in the presence of homogeneous magnetic field. The justification of this approach, based on the work of Saylor and Smolarski,[47] is outlined briefly below.

4.3.2 The Complex Rys Quadrature

In general, there is no three–term recurrence relation that may be applied to generate a set of complex polynomials orthogonal with respect to the standard weighted inner product,

$$\langle p_m(x) | p_n(x) \rangle_w \equiv \int_\gamma p_m(x) \overline{p_n(x)} W(x) \mathrm{d}x = 0, \quad m \neq n, \tag{57}$$

where $\overline{p_n(x)}$ indicates complex conjugation and γ is an arc in the complex plane.[47] However, we can construct a set of *formally orthogonal* (sometimes referred to as *conjugate orthogonal*) polynomials with respect to a bilinear form,

$$[p_m(x) | p_n(x)]_w \equiv \int_\gamma p_m(x) p_n(x) W(x) \mathrm{d}x = 0, \quad m \neq n. \tag{58}$$

As a result, we obtain a tridiagonal complex symmetric Jacobi matrix. The required roots can be calculated as eigenvalues of this matrix, though they are complex.[47] We emphasize that the eigenvectors of the non–Hermitian Jacobi matrix are *not* orthogonal with respect to the standard inner product of Eq. (54), but they are orthogonal with respect to a bilinear form,

$$[\mathbf{v}_i | \mathbf{v}_j] \equiv \sum_k \mathbf{v}_{k,i} \mathbf{v}_{k,j} = 0, \qquad i \neq j. \tag{59}$$

The normalization of the eigenvectors of the Jacobi matrix is as crucial for calculation of the weights of the complex Gauss quadrature as in the real case. We can find a formally orthonormal set of eigenvectors $\{\mathbf{v}_i\}_{i=1}^N$, which form columns of an orthogonal matrix[50] V that satisfies $V^T V = E$, exactly as in the real case. However, for complex eigenvectors this identity implies normalization with respect to the bilinear form, $[\mathbf{v}_i | \mathbf{v}_i] = 1$.

We note that standard eigenvalue solvers such as subroutine `zgeev` from the LAPACK library[51] return eigenvectors that are individually normalized using the standard inner product, the largest component of which are chosen to be real. However, these eigenvectors cannot be made orthonormal with respect to this inner product so they cannot be used in Eq. (55) to find the required weights. We therefore perform an additional normalisation based on the bilinear form above. The whole set then satisfies the condition $V^T V = E$, as in the real case, thus can be used to compute the complex Gauss quadrature weights using standard double precision arithmetic.

For $N < 12$, the recurrence coefficients needed to construct the complex Jacobi matrix can be obtained using the moment method (also known as the Chebyshev algorithm) following the work of Golub and Welsh.[46] We have checked that this method, based on integrating x^n $(n = 1, \ldots, N)$ over the Rys weight, becomes numerically unstable around $N = 12$ both in

case of a real and complex argument Z_{PQ}.

One approach to accommodate the changes in electronic structure induced by the application of a magnetic field is to include a greater number of basis functions of high angular momenta. As a result, we choose to use the modified moment method as outlined by Flocke for real Rys quadrature,[27] which remains numerically stable well beyond $N = 12$. The method uses multiple sets of auxiliary polynomials with known coefficients of their three-term recurrence relation. The choice of the set depends on the size of the argument Z_{PQ}. We have found that we can cover the whole interval relevant for ERIs arising in typical basis sets and magnetic fields up to one atomic unit using the shifted Jacobi polynomials for $|Z_{\mathrm{PQ}}| < 30$ and generalised T-scaled Laguerre polynomials for $|Z_{\mathrm{PQ}}| > 30$. This approach can be used for complex numbers without modifications.

We have found that the absolute value of the complex argument can be considered instead of its positive real component when deciding which set of auxiliary polynomials to use. In case of very large $|Z_{\mathrm{PQ}}|$, it becomes computationally advantageous to use the classical Hermite polynomials,[21] where the roots and weights are be precomputed and rescaled by $\sqrt{|Z_{\mathrm{PQ}}|}$, as this approximation becomes increasingly accurate in the limit of large $|Z_{\mathrm{PQ}}|$. The calculation of the first component of eigenvectors q_0 required to obtain the complex weights is described in Section 3.3; it is simply the zeroth order molecular incomplete gamma function.

Finally, we compare the behaviour of the standard and modified moment methods close to singularities of the elements of the Jacobi matrix as a function of Z_{PQ} in the complex plane, as indicated by Reynolds and Shiozaki[8] for $N = 2$. We observe that the relative error of a test integral utilising the relevant roots and weights does not exceed 10^{-10} when we do not approach the singularity Z^s_{PQ} closer than $|Z_{\mathrm{PQ}} - Z^s_{\mathrm{PQ}}| \sim 10^{-9}$. In practical calculations and testing carried out during this work with field strengths less than 3 atomic units, we have encountered no practical issues associated with such singularities. In the event that such singularities are encountered, the integral batch may be recomputed with a larger number of roots and weights, or using the HGP or MD algorithms.

4.3.3 Vertical Recursion Relation

In the Rys polynomial scheme, the zeroth order terms are not computed from the scaled molecular incomplete gamma function, but from the standard Gaussian pre–factors and the Rys quadrature weights w_λ as

$$\begin{aligned} \mathcal{I}_x\left(0,0;\lambda\right) &= 1.0 \qquad \mathcal{I}_y\left(0,0;\lambda\right) = 1.0 \\ \mathcal{I}_z\left(0,0;\lambda\right) &= U_{\mathrm{PQ}}\sqrt{\frac{4\vartheta}{\pi}}w_\lambda \end{aligned} \tag{60}$$

where the integrand is resolved into the three Cartesian components. For higher order integrals, angular momentum can be incremented using the following recursion relations which are analogous to the HGP vertical recursion relation as shown by Lindh *et. al.*[52]

$$\begin{aligned} \mathcal{I}_i\left(e+1,f;\lambda\right) = &\left\{\mathbf{PA}_i - \frac{\eta t_\lambda^2}{\zeta+\eta}\mathbf{PQ}_i\right\}\mathcal{I}_i\left(e,f;\lambda\right) \\ &+\frac{e}{2\zeta}\left\{1-\frac{\eta t_\lambda^2}{\zeta+\eta}\right\}\mathcal{I}_i\left(e-1,f;\lambda\right) \\ &+\frac{f t_\lambda^2}{2(\zeta+\eta)}\mathcal{I}_i\left(e,f-1;\lambda\right) \\ \mathcal{I}_i\left(e,f+1;\lambda\right) = &\left\{\mathbf{QC}_i + \frac{\zeta t_\lambda^2}{\zeta+\eta}\mathbf{PQ}_i\right\}\mathcal{I}_i\left(e,f;\lambda\right) \\ &+\frac{f}{2\eta}\left\{1-\frac{\zeta t_\lambda^2}{\zeta+\eta}\right\}\mathcal{I}_i\left(e,f-1;\lambda\right) \\ &+\frac{e t_\lambda^2}{2(\zeta+\eta)}\mathcal{I}_i\left(e-1,f;\lambda\right) \end{aligned} \tag{61}$$

where t_λ^2 are the Rys roots, described in Eq. (48). The resolution of the integrand into Cartesian components allows angular momentum to be incremented separately in each direction, resulting in a vertical recursion relation that scales much more favourably with angular momentum than either the MD or HGP algorithms.

4.3.4 Reduced Multiplication Scheme

Integrals suitable for HRR transformation are obtained by multiplying the relevant x, y and

z components of the 2D integrals and summing over the Rys polynomial nodes,

$$[\mathbf{e0}|\mathbf{f0}] = \sum_{\lambda=1}^{N} \mathcal{I}_x\left(e_x, f_x; \lambda\right) \mathcal{I}_y\left(e_y, f_y; \lambda\right) \mathcal{I}_z\left(e_z, f_z; \lambda\right) \quad (62)$$

and subsequently summing over the primitive components of the contracted integral using Eq. (45). This summation step is generally the computational bottleneck of the Rys quadrature approach, scaling less favourably with angular momentum than the comparatively inexpensive VRR. Lindh *et. al.* developed the reduced multiplication scheme;[52] a technique effective at improving the efficiency of this step by maximising the re–use of intermediates and avoiding redundant multiplications.

In the construction of $[\mathbf{e0}|\mathbf{f0}]$ integrals, it was noted that each combination of x and y components was frequently combined with multiple z components, thus creation of an xy intermediate to be combined with many z components in summation over Rys quadrature nodes would reduce the number of individual multiplications required by the number of nodes for each re–use of the intermediate. This is demonstrated by example in Fig. 1.

Aside from the diligent re–use of intermediates, the other main facet of the reduced multiplication scheme is the elimination of superfluous multiplications by unity, discarding $\mathcal{I}_x\left(0, 0; \lambda\right)$ and $\mathcal{I}_y\left(0, 0; \lambda\right)$ from summations where these occur; $\mathcal{I}_z\left(0, 0; \lambda\right)$ cannot be discarded as it carries the Rys weights and other pre–factors. We have employed the reduced multiplication in the generalized Rys quadrature implementation used in this work as it is a useful enhancement to the efficiency of the overall algorithm.

4.4 Cauchy–Schwarz Screening

In addition to the screening of negligible shell–pairs described in subsection 2.1, the Cauchy–Schwarz inequality is exploited to identify and avoid computing negligible batches of integrals,

$$|(\mathbf{ab}|\mathbf{cd})| \leqslant \sqrt{|(\mathbf{ab}|\mathbf{ba})|} \cdot \sqrt{|(\mathbf{cd}|\mathbf{dc})|}. \quad (63)$$

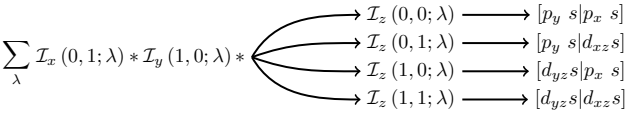

Figure 1: An illustration of how the reduced multiplication scheme can be effective at reducing the amount of computation required. In this example, the 2D integrals in the x and y axes are premultiplied for all λ to form an xy intermediate; this can be combined with four different z components and summed over λ to form four different integrals.

In this work, the threshold for screening at this level is selected to be equal to that for screening individual shell–pairs, 10^{-12}.

5 Assessing the Efficiency of LAO-ERI algorithms

The three ERI algorithms described in Section 4, along with the one–electron integrals of Section 3, have been implemented in the QUEST rapid development platform.[53] This program is written predominantly in the PYTHON language, exploiting just-in-time compilation techniques using the NUMBA compiler.[54,55]

To explore the relative efficiency of the algorithms we consider two example systems, O_2 and C_4H_4. We present relative timings of the integral calculation, broken down by quartet angular momentum, for these systems in both the primitive and contracted form of Dunning's aug-cc-pCVTZ basis set[56] in the spherical harmonic representation. This choice of basis set represents a size typical of that used in production calculations and allows for an assessment of the performance of the integral algorithms over a range of angular momenta.

In Figure 2, integral timings are presented for calculations on the small paramagnetic molecule O_2. These calculations were configured to simulate a uniform external magnetic field of 1 atomic unit, perpendicular to the bonding axis, on the electronic state corresponding to lowest energy component of the triplet ground state of O_2 at zero–field. The

left–hand panel of Figure 2 shows the timings pertaining to the primitive basis set, whilst the right–hand panel shows the corresponding data for the contracted basis set.

In the presence of a strong magnetic field, the electron density of the system is compressed in an anisotropic manner, with the compression perpendicular to the field being more pronounced than that in the direction of the applied field, as described for example in Refs. 4,10,11. These changes are however small relative to the changes in density upon formation of a typical covalent bond and so a simple approach to introduce sufficient flexibility into the basis set to adequately accommodate these effects is to un–contract the basis functions. The development of basis sets tailored to finite field calculations has not yet been pursued, however for such sets, contracted functions could be developed to enhance computational efficiency. In Figure 2 we also therefore present timings for the aug-cc-pCVTZ basis set in its contracted form, where the contractions used are those defined for zero–field calculations.

In this work, we have only considered fields of up to ~ 1 atomic unit in strength, equivalent to $235'000$ Tesla. For the purposes of checking the numerical stability of the implemented code, some additional calculations were undertaken with fields of up to ~ 3 atomic units in strength. We note however that, at field strengths greater than a few atomic units, the use of anisotropic basis sets may become necessary,[57,58] along with a more careful consideration of non Born–Oppenheimer corrections.[59]

The timings for the primitive basis for O_2 in the left hand panels of Figure 2 are classified by the total angular momentum of the shell quartet, $L_{\text{bra}} + L_{\text{ket}}$. In the upper panel, the average CPU time per integral in each class is presented; this gives a system independent measure of the performance of each algorithm for the different classes of integral. As would be expected from subsection 4.1, the MD algorithm exhibits the least favourable performance overall. The time per integral for the MD algorithm is little different from that of the HGP algorithm for very low angular momenta of $\lesssim 2$, perhaps having a marginal advantage over HGP for these classes, however the time per integral for MD rapidly begins to exceed that of HGP for classes of increasing angular momenta. This is a result of the recursion relation of Eq. (41) having twice the number of terms and indices as its zero–field counterpart, effectively eliminating a principle advantage of the MD algorithm whilst retaining the principle disadvantage in the form of Eq. (42), leading to the relatively poor scaling with angular momentum observed here.

The HGP algorithm delivers a superior performance to the MD algorithm for integrals of angular momenta above the range $\lesssim 2$. This is unsurprising because, whilst the VRR of Eq. (44) has one term more than the MD recursion relation, the HRR of Eq. (7) is much simpler than the transformation stage of the MD algorithm, Eq. (42). In essence, the HGP algorithm for LAO-ERIs is little different to that over standard GTOs, thus retains many of its well documented comparative advantages.[28,60]

A shortcoming that both the MD and HGP algorithms share is that their efficiency begins to deteriorate when the total angular momentum of the integral increases further, exceeding ~ 5 for primitive functions. It is clear from Figure 2 however that the Rys quadrature scheme performs significantly better than either the MD or HGP algorithms for integrals with angular momentum $\gtrsim 5$, becoming increasingly advantageous with higher total angular momentum. This trend can be understood by comparing the HGP VRR of Eq. (44) and the Rys VRR of Eq. (61); in the Rys scheme recursion is applied to the integrand polynomial, which is separable by Cartesian components allowing angular momentum to be incremented in each component independently and resulting is a much lower scaling with angular momentum than the HGP VRR, where the intermediate auxiliary integrals are non–separable. The scaling of the Rys summation step of Eq. (62), the steepest scaling part of the Rys algorithm, is minimised by application of the reduced multiplication scheme as described in subsection 4.3.4.

In contrast it can also be seen in Figure 2 that the Rys algorithm is the least efficient for computing ERIs of very low total angular momen-

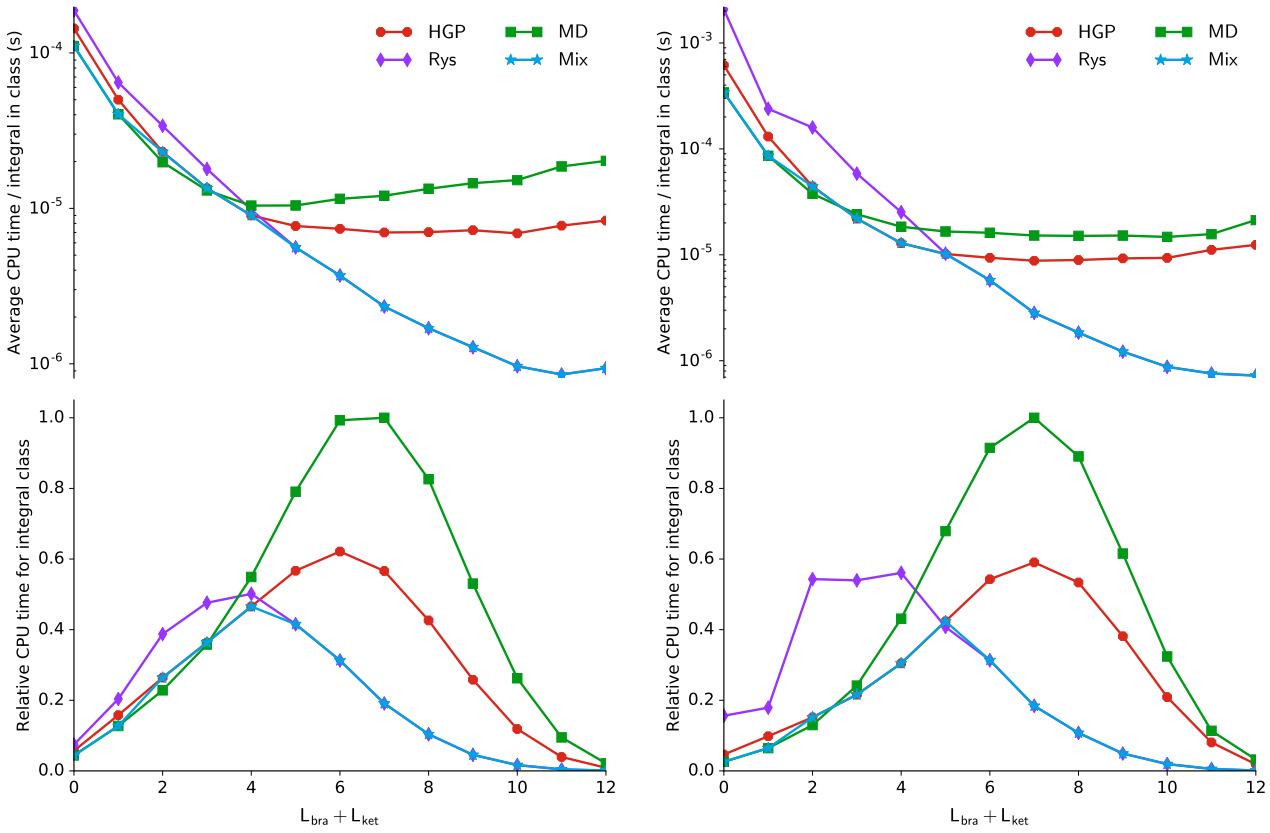

Figure 2: Relative timings for LAO-ERIs in a calculation on the O_2 molecule in the aug-cc-pCVTZ basis, classified according to the total angular momenta $L_{\text{bra}} + L_{\text{ket}}$ for each shell quartet. The left hand panels show the results for the primitive basis, the right hand panels for the contracted basis set.

tum, being in this case inferior to both MD and HGP. This is because the zeroth–order terms of the MD and HGP algorithms are simply scaled molecular incomplete gamma functions and are relatively inexpensive to compute, whereas the zeroth–order terms of the Rys algorithm requires the more computationally expensive calculation of quadrature nodes and weights. For integrals of low angular momentum, computing the zeroth–order term is generally the dominant step, thus the pre–factor is greater for the Rys quadrature than for the MD or HGP algorithms, impairing the performance of the Rys scheme at low angular momenta.

In the lower panel of Figure 2, the relative CPU time for each integral class in the calculation is presented; this plot reflects not only the angular momenta of integrals present but also their relative distribution as determined by the particular choice of basis and the system under study. It is again clear that he MD approach is the least efficient, with the largest amount of time spent on integrals with $L_{\text{bra}} + L_{\text{ket}} = 7$, the HGP algorithm delivers a considerable improvement for $L_{\text{bra}} + L_{\text{ket}} > 4$, and is comparable with MD for lower angular momenta integrals. For the HGP approach, the most time is spent on integrals with $L_{\text{bra}} + L_{\text{ket}} = 6$. Most striking is the significant improvement offered by the use of Rys quadrature for $L_{\text{bra}} + L_{\text{ket}} > 4$, with the largest amount of time being spent on integrals with $L_{\text{bra}} + L_{\text{ket}} = 4$ for this approach. Furthermore, as would be anticipated from the above discussion, for $L_{\text{bra}} + L_{\text{ket}} < 4$ the Rys approach is noticeably less efficient than either the MD or HGP schemes.

In the right hand panels of Figure 2, the corresponding analysis is presented for the contracted aug-cc-pCVTZ basis. Qualitatively the plots are similar, however, there are some important differences. Consistent with the discussion in Section 4.2, the HGP algorithm is

particularly efficient for contracted basis sets since its HRR may be applied to contracted integrals. This effect can be discerned in the upper right plot of Figure 2, noting that the HGP algorithm becomes more efficient than MD earlier at $L_{\text{bra}} + L_{\text{ket}} = 2$. On the other hand, the efficiency of the Rys quadrature calculations is adversely effected by contraction, as it necessitates multiple sets of quadrature roots and weights to be computed per integral batch; this effect can be discerned from the upper right plot, noting a later crossover with HGP at $L_{\text{bra}} + L_{\text{ket}} = 5$, beyond which the Rys quadrature again becomes the most efficient technique.

A similar analysis has been conducted for the cyclobutadiene molecule, C_4H_4, at the same geometry as used in Ref. 1 with a uniform magnetic field of strength 1 atomic unit perpendicular to the molecular plane. The results pertaining to the C_4H_4 molecule are presented in Figure 3. The upper panels showing the system independent plots are remarkably similar to those for O_2, confirming the use of this measure for assessing the efficiency of the different algorithms. In particular, the crossover values at which different methods become the most efficient are remarkably transferrable. The lower panels are also very similar, reflecting similar types of functions contributing to the basis set. We have confirmed that increasing the cardinal number of the Dunning-type basis set does not significantly affect conclusions on the relative efficiency of the approaches considered and that the system independent plots (upper panels) remain broadly system independent.

Given that the crossovers in performance between the algorithms are remarkably transferrable, we have considered a simple mixed approach to achieve the optimal efficiency in evaluating the LAO-ERIs. In all constituent plots of Figures 2 and 3, the results of the mixed approach are plotted with line style $\star$–$\star$. In our integral evaluation code, we have introduced a simple function to select the most appropriate algorithm based on the overall contraction length and the value of $L_{\text{bra}} + L_{\text{ket}}$. After testing over a range of systems we select the MD, HGP and Rys algorithms based on these values according to Table 1. This approach can be highly effective in reducing overall computation time, compared with the exclusive use of any one of the algorithms, often with savings between 10% and 30%. The largest gains using the mixed approach are apparent when using contracted functions (see e.g. the lower right panels of Figures 2 and 3). It is interesting to note that all three approaches considered contribute to the mixed scheme, with MD being most efficient for the lowest angular momenta integrals, Rys quadrature the most efficient for the high angular moment integrals and HGP being optimal in the intermediate region. We expect the simple heuristics used in the mixed approach here to be transferrable to many common basis sets where contraction is most significant in the lower angular momenta core functions. However, some re–calibration may of course be necessary for basis sets containing functions with significantly greater contraction lengths than tested in this work.

Table 1: Ranges of $L_{\text{bra}} + L_{\text{ket}}$ in which each of the considered integral algorithms may be considered optimal. These values are used for the construction of a mixed scheme (see text for details).

	MD	HGP	Rys
Primitive	0–1	2–4	5+
Contracted	0–1	2–5	6+

6 Conclusions

The implementation of integral schemes for non-perturbative electronic structure calculations in the presence of strong magnetic fields using LAOs has been presented. The impact of the use of LAOs on the complexity of three LAO-ERI algorithms was discussed in detail. For the MD method, the introduction of LAOs leads to a significant increase in complexity and has a negative impact on its overall efficiency, particularly for integrals over higher angular momenta basis functions. However, the method still retains efficiency for integrals involving only the lowest angular momenta functions. For the HGP method, the introduction

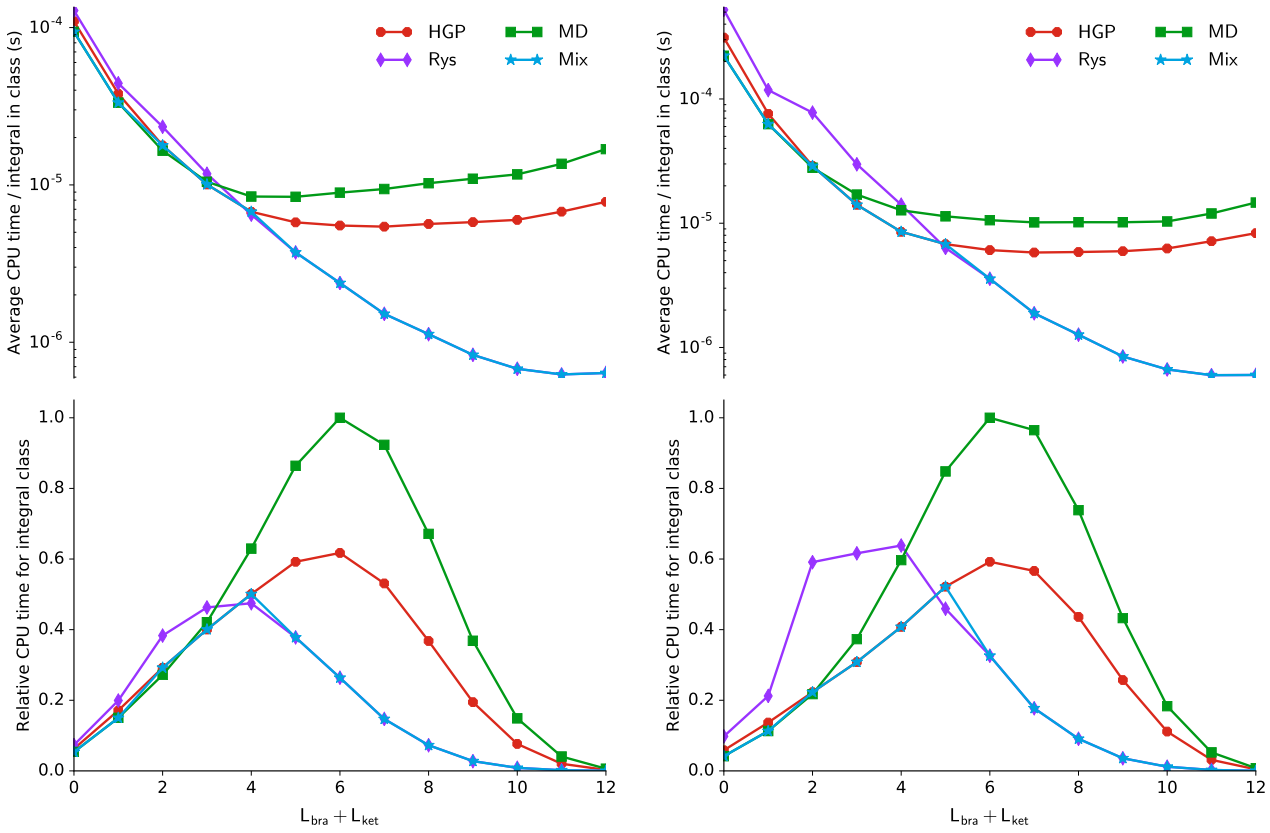

Figure 3: Relative timings for LAO-ERIs in a calculation on the C_4H_4 molecule in the aug-cc-pCVTZ basis, classified according to the total angular momenta $L_{\text{bra}} + L_{\text{ket}}$ for each shell quartet. The left hand panels show the results for the primitive basis, the right hand panels for the contracted basis set.

of LAOs does not significantly complicate the underlying algorithm and the efficiency of the HGP scheme for contracted basis functions remains a significant advantage in the generalized form.

For the Rys quadrature approach, a careful approach is required to extend the method to the complex case required for LAO integrals. In contrast with previous implementations, we use Flocke's approach[27] rather than an interpolation scheme for the roots and weights, avoiding the need to construct and store large interpolation tables.[8] We also find that the computation of the roots and weights on the fly can be carried out with standard double precision arithmetic. The reduced multiplication scheme of Lindh[52] was adopted in this context to further improve the efficiency of the summation step. One potential complicating factor for the application of Rys quadrature in this context is the possibility of encountering singularities in the complex plane.[8,47] Whilst we have confirmed that these are still present with use of the alternative algorithms presented here, we have not encountered difficulties due to these in any practical calculations, including tests with molecules at a wide range of geometries with fields up to 3 atomic units in strength. In our implementation, if such problems are detected the evaluation of the integral batch can be repeated automatically with a larger number of roots and weights or with one of the alternative LAO-ERI algorithms.

A simple mixed approach was designed to exploit the different advantages of the LAO-ERI algorithms. Specifically, Rys quadrature is used for high angular momenta integrals, the HGP algorithm is used for intermediate angular momenta integrals and particularly where contracted functions are employed and the MD method is employed for the lowest angular momenta integrals. When combined, the mixed

approach can achieve substantial efficiencies in overall computation compared with the exclusive use of any one integral algorithm. This provides a robust approach for calculating LAO molecular integrals over a very broad range of fields in an efficient manner, enabling the efficient implementation of non-perturbative treatments of strong magnetic fields in electronic structure calculations. In future work, we will consider the evaluation of geometrical derivatives of these integrals in a similar fashion to enable the efficient calculation of molecular gradients and optimized geometries in the presence of strong magnetic fields.

Acknowledgements

The authors are grateful for support from the Engineering and Physical Sciences Research Council (EPSRC), Grant No. EP/M029131/1. AMT gratefully acknowledges support from the Royal Society University Research Fellowship scheme.

References

(1) Tellgren, E. I.; Soncini, A.; Helgaker, T. Nonperturbative ab initio calculations in strong magnetic fields using London orbitals. *J. Chem. Phys.* **2008**, *129*, 154114.

(2) Tellgren, E. I.; Helgaker, T.; Soncini, A. Non-perturbative magnetic phenomena in closed-shell paramagnetic molecules. *Phys. Chem. Chem. Phys.* **2009**, *11*, 5489.

(3) Tellgren, E. I.; Reine, S. S.; Helgaker, T. Analytical GIAO and hybrid-basis integral derivatives: application to geometry optimization of molecules in strong magnetic fields. *Phys. Chem. Chem. Phys.* **2012**, *14*, 9492.

(4) Lange, K. K.; Tellgren, E. I.; Hoffmann, M. R.; Helgaker, T. A Paramagnetic Bonding Mechanism for Diatomics in Strong Magnetic Fields. *Science* **2012**, *337*, 327–331.

(5) Tellgren, E. I.; Fliegl, H. Non-perturbative treatment of molecules in linear magnetic fields: Calculation of anapole susceptibilities. *J. Chem. Phys.* **2013**, *139*, 164118.

(6) Tellgren, E. I.; Teale, A. M.; Furness, J. W.; Lange, K. K.; Ekström, U.; Helgaker, T. Non-perturbative calculation of molecular magnetic properties within current-density functional theory. *J. Chem. Phys.* **2014**, *140*, 034101.

(7) Reimann, S.; Ekström, U.; Stopkowicz, S.; Teale, A. M.; Borgoo, A.; Helgaker, T. The importance of current contributions to shielding constants in density-functional theory. *Phys. Chem. Chem. Phys.* **2015**, *17*, 18834–18842.

(8) Reynolds, R. D.; Shiozaki, T. Fully relativistic self-consistent field under a magnetic field. *Phys. Chem. Chem. Phys.* **2015**, *17*, 14280–14283.

(9) Stopkowicz, S.; Gauss, J.; Lange, K. K.; Tellgren, E. I.; Helgaker, T. Coupled-cluster theory for atoms and molecules in strong magnetic fields. *J. Chem. Phys.* **2015**, *143*, 074110.

(10) Furness, J. W.; Verbeke, J.; Tellgren, E. I.; Stopkowicz, S.; Ekström, U.; Helgaker, T.; Teale, A. M. Current Density Functional Theory Using Meta-Generalized Gradient Exchange-Correlation Functionals. *J. Chem. Theory Comput.* **2015**, *11*, 4169–4181.

(11) Furness, J. W.; Ekström, U.; Helgaker, T.; Teale, A. M. Electron localisation function in current-density-functional theory. *Mol. Phys.* **2016**, *114*, 1415–1422.

(12) Hampe, F.; Stopkowicz, S. Equation-of-motion coupled-cluster methods for atoms and molecules in strong magnetic fields. *J. Chem. Phys.* **2017**, *146*, 154105.

(13) London, F. Théorie quantique des courants interatomiques dans les combinaisons aromatiques. *J. Phys. Radium* **1937**, *8*, 397–409.

(14) Ditchfield, R. Self-consistent perturbation theory of diamagnetism. *Mol. Phys.* **1974**, *27*, 789–807.

(15) Obara, S.; Saika, A. Efficient recursive computation of molecular integrals over Cartesian Gaussian functions. *J. Chem. Phys.* **1986**, *84*, 3963.

(16) Honda, M.; Sato, K.; Obara, S. Formulation of molecular integrals over Gaussian functions treatable by both the Laplace and Fourier transforms of spatial operators by using derivative of Fourier-kernel multiplied Gaussians. *J. Chem. Phys.* **1991**, *94*, 3790.

(17) Kiribayashi, S.; Kobayashi, T.; Nakano, M.; Yamaguchi, K. Self-consistent-field calculations of molecular magnetic properties using gauge-invariant atomic orbitals. *Int. J. Comput. Theor. Chem.* **1999**, *75*, 637–643.

(18) Ishida, K. ACE algorithm for the rapid evaluation of the electron-repulsion integral over Gaussian-type orbitals. *Int. J. Comput. Theor. Chem.* **1996**, *59*, 209–218.

(19) Ishida, K. Molecular integrals over the gauge-including atomic orbitals. *J. Chem. Phys.* **2003**, *118*, 4819.

(20) Dupuis, M. Evaluation of molecular integrals over Gaussian basis functions. *J. Chem. Phys.* **1976**, *65*, 111.

(21) King, H. F.; Dupuis, M. Numerical integration using rys polynomials. *J. Comput. Phys.* **1976**, *21*, 144–165.

(22) McMurchie, L. E.; Davidson, E. R. One- and two-electron integrals over cartesian gaussian functions. *J. Comput. Phys.* **1978**, *26*, 218–231.

(23) Tachikawa, M.; Shiga, M. Evaluation of atomic integrals for hybrid Gaussian type and plane-wave basis functions via the McMurchie-Davidson recursion formula. *Phys. Rev. E* **2001**, *64*, 056706.

(24) Kuchitsu, T.; Okuda, J.; Tachikawa, M. Evaluation of molecular integral of Cartesian Gaussian type basis function with complex-valued center coordinates and exponent via the McMurchie-Davidson recursion formula, and its application to electron dynamics. *Int. J. Comput. Theor. Chem.* **2009**, *109*, 540–548.

(25) LONDON, A quantum chemistry program for plane–wave/GTO hybrid basis sets and finite magnetic field calculations. `londonprogram.org`.

(26) BAGEL, Brilliantly Advanced General Electronic-structure Library. `nubakery.org`, Published under the GNU General Public License.

(27) Flocke, N. On the use of shifted Jacobi polynomials in accurate evaluation of roots and weights of Rys polynomials. *J. Chem. Phys.* **2009**, *131*, 064107.

(28) Gill, P. M. *Adv. Quantum Chem.*; Elsevier BV, 1994; pp 141–205.

(29) Gill, P. M. W.; Johnson, B. G.; Pople, J. A.; Taylor, S. W. Modeling the potential of a charge distribution. *J. Chem. Phys.* **1992**, *96*, 7178–7179.

(30) Head-Gordon, M.; Pople, J. A. A method for two–electron Gaussian integral and integral derivative evaluation using recurrence relations. *J. Chem. Phys.* **1988**, *89*, 5777.

(31) Rys, J.; Dupuis, M.; King, H. F. Computation of electron repulsion integrals using the Rys quadrature method. *J. Comput. Chem.* **1983**, *4*, 154–157.

(32) Johnson, B. G.; Gill, P. M.; Pople, J. The efficient transformation of (m0|n0) to (ab|cd) two-electron repulsion integrals. *Chem. Phys. Lett.* **1993**, *206*, 229–238.

(33) Makowski, M. Simple yet powerful techniques for optimization of horizontal recursion steps in Gaussian-type two-electron integral evaluation algorithms.

Int. J. Comput. Theor. Chem. **2006**, *107*, 30–36.

(34) Ryu, U.; Lee, Y. S.; Lindh, R. An efficient method of implementing the horizontal recurrence relation in the evaluation of electron repulsion integrals using Cartesian Gaussian functios. *Chem. Phys. Lett.* **1991**, *185*, 562–568.

(35) Schlegel, H. B.; Frisch, M. J. Transformation between Cartesian and pure Spherical harmonic Gaussians. *Int. J. Comput. Theor. Chem.* **1995**, *54*, 83–87.

(36) Obara, S.; Saika, A. General recurrence formulas for molecular integrals over Cartesian Gaussian functions. *J. Chem. Phys.* **1988**, *89*, 1540.

(37) Shavitt, I. In *Methods Comput. Phys.*; Alder, B., Fernbach, S., Rotenberg, M., Eds.; Academic Press New York, 1963; Vol. 3; pp 1–45.

(38) Saunders, V. R. *Computational Techniques in Quantum Chemistry and Molecular Physics*; Springer Netherlands, 1975; pp 347–424.

(39) Boys, S. F. Electronic Wave Functions. I. A General Method of Calculation for the Stationary States of Any Molecular System. *Proc. R. Soc. A* **1950**, *200*, 542–554.

(40) Helgaker, T.; Jørgensen, P.; Olsen, J. *Molecular Electronic-Structure Theory*; John Wiley & Sons, Ltd, 2000.

(41) Čársky, P.; Polášek, M. Incomplete GammaFm(x) Functions for Real Negative and Complex Arguments. *J. Comput. Phys.* **1998**, *143*, 259–265.

(42) Mathar, R. J. Numerical Representations of the Incomplete Gamma Function of Complex-Valued Argument. *Numerical Algorithms* **2004**, *36*, 247–264.

(43) Ishida, K. Accurate and fast algorithm of the molecular incomplete gamma function with a complex argument. *J. Comput. Chem.* **2004**, *25*, 739–748.

(44) Colle, R.; Fortunelli, A.; Simonucci, S. A mixed basis set of plane waves and Hermite Gaussian functions. Analytic expressions of prototype integrals. *Il Nuovo Cimento D* **1987**, *9*, 969–977.

(45) Colle, R.; Fortunelli, A.; Simonucci, S. Hermite Gaussian functions modulated by plane waves: a general basis set for bound and continuum states. *Il Nuovo Cimento D* **1988**, *10*, 805–818.

(46) Golub, G. H.; Welsch, J. H. Calculation of Gauss quadrature rules. *Mathematics of Computation* **1969**, *23*, 221–221.

(47) Saylor, P. E.; Smolarski, D. C. *Numerical Algorithms* **2001**, *26*, 251–280.

(48) Wilf, H. S. *Mathematics for the physical sciences*; John Wiley and Sons Inc, 1962.

(49) Sack, R. A.; Donovan, A. F. An algorithm for Gaussian quadrature given modified moments. *Numerische Mathematik* **1971**, *18*, 465–478.

(50) Horn, R. A.; Johnson, C. R. *Matrix analysis*; Cambridge University Press, 1985.

(51) Dongarra, J. J.; Demmel, J. W.; Ostrouchov, S. *Computational Statistics*; Physica-Verlag HD, 1992; pp 23–28.

(52) Lindh, R.; Ryu, U.; Liu, B. The reduced multiplication scheme of the Rys quadrature and new recurrence relations for auxiliary function based two-electron integral evaluation. *J. Chem. Phys.* **1991**, *95*, 5889.

(53) QUEST, A rapid development platform for Quantum Electronic Structure Techniques. 2017.

(54) Numba. `numba.pydata.org`, 2017; Version 0.32.

(55) Lam, S. K.; Pitrou, A.; Seibert, S. Numba. Proceedings of the Second Workshop on the LLVM Compiler Infrastructure in HPC - LLVM'15. 2015.

(56) Kendall, R. A.; Dunning, T. H.; Harrison, R. J. Electron affinities of the first-row atoms revisited. Systematic basis sets and wave functions. *J. Chem. Phys.* **1992**, *96*, 6796–6806.

(57) Schmelcher, P.; Cederbaum, L. S. Molecules in strong magnetic fields: Properties of atomic orbitals. *Phys. Rev. A* **1988**, *37*, 672–681.

(58) Kubo, A. The Hydrogen Molecule in Strong Magnetic Fields: Optimizations of Anisotropic Gaussian Basis Sets. *J. Phys. Chem. A* **2007**, *111*, 5572–5581.

(59) Adamowicz, L.; Tellgren, E. I.; Helgaker, T. Non-Born–Oppenheimer calculations of the HD molecule in a strong magnetic field. *Chem. Phys. Lett.* **2015**, *639*, 295–299.

(60) Gill, P. M. W.; Pople, J. A. The PRISM algorithm for two–electron integrals. *Int. J. Comput. Theor. Chem.* **1991**, *40*, 753–772.

TOC Graphic

For table of contents only.